Lifetime Measurements with a Scanning Positron Microscope

A. David, G. Kögel, P. Sperr, and W. Triftshäuser
Institut für Nukleare Festkörperphysik, Universität der Bundeswehr München, 85577 Neubiberg, Germany
(Received 26 February 2001; published 19 July 2001)

First lifetime results obtained with a scanning positron microscope will be presented. A pulsed positron beam with a variable energy from 0.5 to 20 keV, with a spot diameter of 2 μm, can be electronically scanned over an area of 0.6×0.6 mm^2. This beam is formed after a double-stage stochastic cooling (moderation) of positrons emitted from a radioactive isotope. Included in the system is a conventional scanning electron microprobe for surface analysis. Three-dimensional positron lifetime spectra of a GaAs sample with a small surface scratch reveal the range due to the mechanical damage.

DOI: 10.1103/PhysRevLett.87.067402 PACS numbers: 78.70.Bj, 07.78.+s, 41.75.Fr, 61.72.Ji

Positrons are very sensitive probes for vacancy-type defects of atomic dimensions, e.g., vacancies, vacancy agglomerates, voids, dislocations, or inner surfaces. It is well established that positrons can be trapped at these defects and because of the locally reduced electron density the lifetime of the positron localized at the defect increases. This lifetime has characteristic values for each specific defect type. Since it is possible to determine up to four different lifetimes at their corresponding intensities from an experimentally measured lifetime spectrum, various atomic defect configurations and concentrations which may be present simultaneously can be separated out with very high sensitivity ($\sim$1 ppm) and in a nondestructive way.

The conventional lifetime method using positrons directly from a radioactive isotope (positron energies up to about 600 keV) and hence ranges in solids of several hundred micrometers can give information for defect distributions of macroscopic regions or of an average defect structure. Monoenergetic positrons of low and variable energy (1 to 20 keV), however, can sample near surface regions and layered structures in a much more detailed manner. By varying the positron energy, the maximum range of the positrons can be controlled and various depth regions can be studied. Furthermore, with a pulsed positron beam, lifetime studies as a function of the positron energy are possible [1–3]. With such a pulsed system and a positron beam diameter of about 3 mm, planar pure surfaces, coated and laser treated surfaces of metals, alloys, and semiconductors, as well as ion implanted materials have been and are being studied [4–8]. With this depth profiling interfaces in semiconductors, oxides, and metals can also be investigated [9].

The typical textures of technical alloys or the dimensions of functional units in microelectronic devices, however, are in the range of micrometers. Therefore, for many applications and investigations in materials science, a positron beam diameter in the micrometer range is desirable and necessary. This leads to a scanning positron microscope (SPM) consisting of a pulsed positron beam ($\sim$1 μm diameter) of variable energy with a scanning facility of the beam [10–12].

The fundamental difference between electron and positron microbeams consists in the flux density of its sources. The flux density of a typical electron source exceeds the flux density of a monoenergetic positron source by many orders of magnitude. Therefore the probe forming strategy for a scanning positron microscope must be to maintain the positron flux as much as possible, in contrast to the typical probe forming strategy for a scanning electron microscope which is based on narrow apertures and corresponding allowable intensity losses. Therefore, in order to obtain a sufficient event rate with a relative weak and easy to handle primary positron source, the design is based on only one remoderation stage in reflection mode. Furthermore, the development had to focus on very critical problems, i.e., sufficient spatial and time resolution, very good mechanical and electronic stability, ultrahigh vacuum conditions, and an appropriate specimen chamber.

The principle of the design of the SPM is shown schematically in Fig. 1. The complete system is described in Refs. [11,12]. Specimens of dimensions up to $20 \times 20 \times 3$ mm^3 can be inserted through a lock system. Any region of the specimen can be positioned with a manipulator within the electronically scanned area of at least 600×600 μm^2. Besides the positron beam, an electron beam is provided which produces a conventional electron image of the specimen surface, and regions of interest can then be selected for the investigation with positrons.

The source-moderator assembly, coupled with a first accelerator, produces a continuous positron beam of 20 eV kinetic energy. This beam is injected into the drift tube where a sawtooth voltage of 50 MHz is applied. Positrons in each 20 ns segment of the continuous beam are in this way compressed into bunches of approximately 2 ns width. After leaving the drift space the positrons are accelerated and injected into a 100 MHz sine wave buncher which reduces the pulse width to about 200 ps. A beam blanker, positioned in front of the buncher, suppresses the time-uncorrelated background due to positrons outside of the prebunched pulse. With an average energy of 5 keV the positrons are then focused onto the remoderator, i.e., a single crystal of tungsten. From the resulting spot size of

 © 2001 The American Physical Society

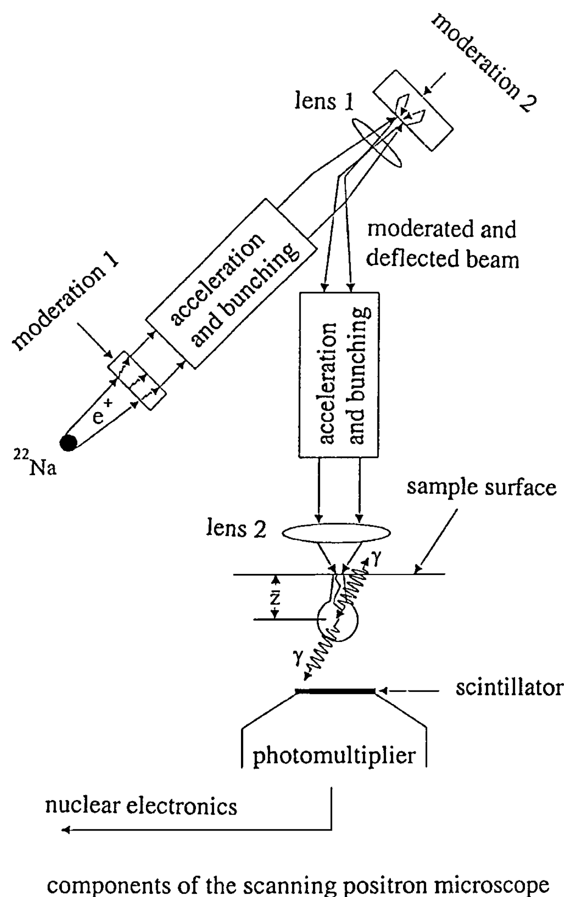

FIG. 1. Schematic principle of the scanning positron microscope. $\bar{z}$ is the mean implantation depth of the positrons.

less than 20 μm the positrons are reemitted with a measured efficiency of (23 $\pm$ 2)%. They are deflected into the optical column for final acceleration and are directed to the magnetic field of the probe-forming lens very close to the target position.

Because of the completely different measuring technique with positrons, this part of the SPM must differ completely from the specimen chamber of a scanning electron microscope. In order to obtain a good time resolution and a high count rate of the annihilation photons, a radiation detector as large as meaningful is positioned as close as possible to the specimen, respectively. On the other hand, the half space in front of the specimen has to be free of matter in order to suppress possible distortions of the lifetime spectra by annihilation radiation resulting from backscattered positrons annihilating at the wall of the vacuum system. The necessary design requirements have been met by a side-gap single-pole lens, placed behind the specimen just outside of the vacuum chamber with the radiation detector inside the central pole shoe [13]. A specially shaped BaF_2 scintillator crystal, coupled to a XP 2020Q photomultiplier, is used as detector for the 511 keV photons.

With the remoderation efficiency of about 23%, the phase-space density of the reemitted positrons will exceed the one of the first moderator by a factor of about 3×10^5. Up to now, the typical gain in phase-space density of a single remoderation stage was only about 20 [14]. This means that in the design of this SPM, only one remoderation stage will replace three conventional remoderation stages, thereby reducing the required primary source strength by a factor of 25. This progress is due to the well-balanced beam-transport system, the superior properties of the single-pole lens as well as the application of time bunching, which contributes with a factor of more than 50 to the total gain in the phase-space density [12].

The electron beam which passes the same optical column as the positron beam is used, because of its much higher intensity, for perfect focusing and alignment of the beam at the target position. From the surface image obtained with the electron beam, regions of interest can be selected for the positron beam investigations.

Results of the electron beam image of a test specimen are shown in Fig. 2. A platinum pattern is evaporated onto the SiO_2 layer of a silicon wafer. From a line scan (fixed y coordinate, variable x coordinate as indicated) an electron beam diameter of 0.5 μm (FWHM) is determined.

For the positron beam mode, the potentials at the target and in the optical column have to be reversed. After this change, the center of both beams coincides within about 30 μm. The three-dimensional positron lifetime image of the same test specimen is shown in Fig. 3. The image consists of 20×20 pixels. For each pixel the measuring time for the positron lifetime spectrum was 140 s with a primary source activity of 30 mCi ^{22}Na. The positron mean lifetime is plotted as a function of the x and y dimensions. For the area covered with platinum the mean lifetime is 190 ps, for SiO_2 the mean lifetime is 350 ps. Both lifetimes are larger as compared to their perfect materials. This increase is due to defects in the respective layers, originating from the production process. From the line scan a dimension of 2 μm (FWHM) for the positron beam

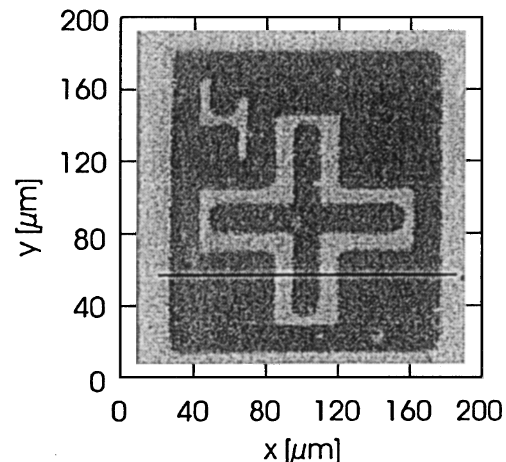

FIG. 2. Electron beam image of the surface of a test chip. The light area is SiO_2, and the dark area is platinum. The electron energy is 8 keV.

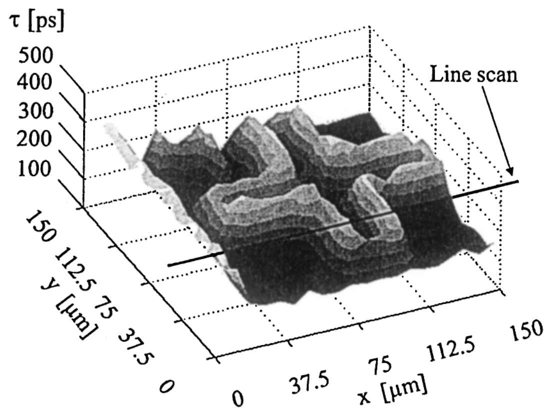

FIG. 3. Positron beam image of the same test chip as of Fig. 2. The mean positron lifetime is plotted as a function of the x and y dimensions. The coordinates of the line scan are indicated. The positron energy is 8 keV.

is determined, which is the best spatial resolution obtained so far.

With a reduced spatial resolution of about 5 μm of the positron beam, however, higher count rate measurements were performed on a GaAs wafer where the surface has been scratched with a sharp diamond needle. Figure 4 shows an image of part of the scratch as obtained with a light microscope, with the electron microbeam and with the positron beam, respectively. The images from the light microscope and from the electron microbeam agree very well and reveal the visible dimensions of the scratch to ~1.2 mm in length and around 75 μm in width. The image of the positron beam is taken at a positron energy of 17 keV with 19 steps in the x direction (step width 21.6 μm) and 20 steps in the y direction (step width 9.4 μm), i.e., 400 lifetime spectra at 800 s each. The count rate was about 100 counts/s.

The most interesting and very surprising result of the positron lifetime measurements is the observed long mean lifetime at the area along the direction of the scratch where no surface damage is visible. For comparison, we quote relevant positron lifetimes in GaAs from a recent review [15], i.e., 230 ps in the bulk, 255–295 ps at monovacancies, and 400–500 ps in voids. Depending on the plastic strain, 270–500 ps are observed in deformed GaAs [15]. Thus the long positron lifetime of about 330 ps is evidence of plastic strain or vacancy clusters close to the surface in a region where no surface damage is visible. Possibly the stress by the diamond needle was gradually increased in front of the scratch so that a plastic deformation occurred before the surface was actually scratched.

Furthermore, at different positron energies a line scan (74 steps with a step width of 3.15 μm) has been performed perpendicular to the scratch at a distance of about 350 μm from its tip (Fig. 5). Each lifetime spectrum contains about 10^4 events. At all positron energies the dimension of the scratch (~75 μm) is clearly indicated. The defects introduced by the mechanical damage are

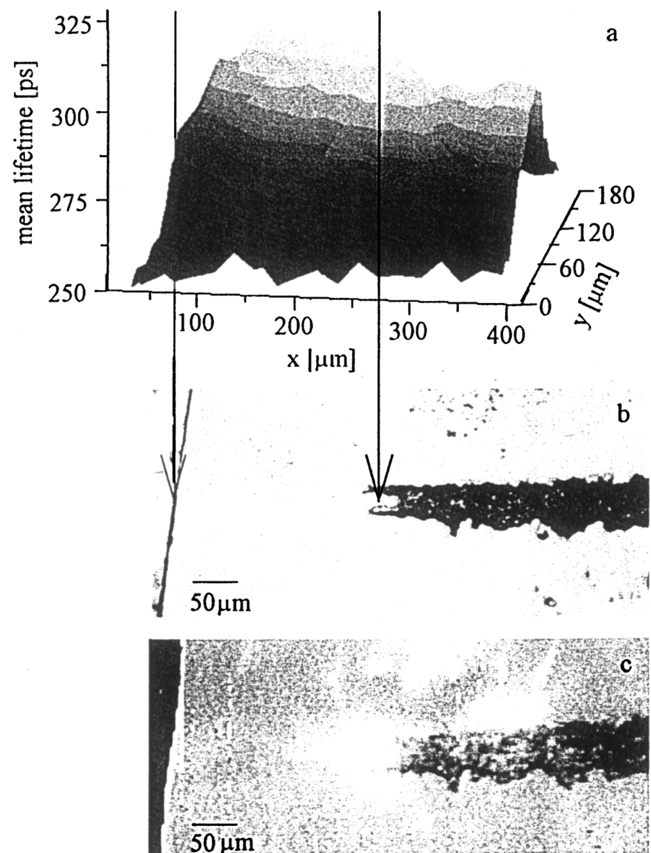

FIG. 4. Image of the GaAs wafer (scratched and unscratched area) as obtained with a light microscope (b), with the electron microbeam (c), and from the lifetime results of the positron microbeam (a). Incident energies of the electron and positron beam are 12 and 17 keV, respectively. The frames are aligned by means of the edge of a Pt foil which can be identified in all three images (left arrow). The right arrow points to the tip of the scratch.

obviously restricted mainly to this area. The mean lifetime decreases from 360 ps at 5 keV to 245 ps at 17 keV which is due to the influence of the surface. But even at 17 keV, which corresponds to a mean implantation depth of 0.7 μm, there are still dominating vacancylike defects present within the scratched region only.

Outside the damaged region one observes the typical monotonic transition of the mean positron lifetime from the extrapolated surface value of about 400 ps to the bulk value of about 230 ps [15]. This transition is due to partial back diffusion from the bulk to the surface. The extrapolated surface value agrees very well with recently published data [16].

Within the damaged region there must be large vacancy clusters at least in the region from the surface to the mean positron implantation depth at 17 keV, i.e., about 0.7 μm. The dependence of the mean positron lifetime on the implantation energy can be attributed to a depth dependence of either the size or the concentration of these defects. The statistical quality of our present data set is not quite sufficient for a quantitative analysis, but it is more than

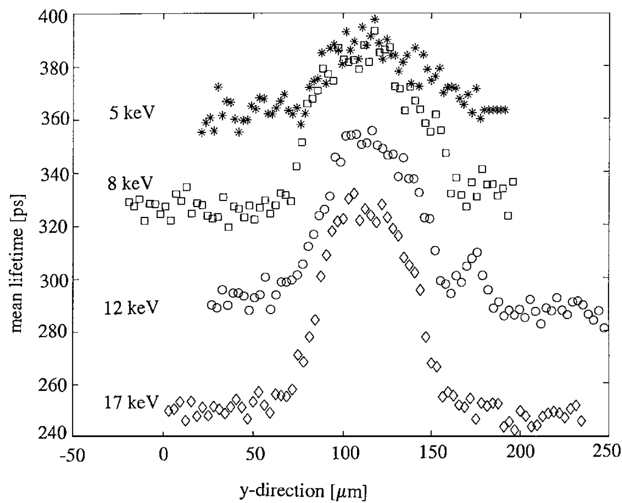

FIG. 5. Line scans of the positron microbeam, perpendicular to the scratch, are shown for different incident positron energies. The mean positron lifetime is plotted as a function of position and of positron energy.

adequate to exclude artifacts of the analysis as the origin of the reported lifetime distributions, because all lifetime spectra have been analyzed under identical conditions, and since the observed total variation of the mean lifetime is about 50 times larger than the statistical uncertainty of the individual mean lifetimes. However, with a more intense positron source a better statistical accuracy of the data can be achieved and up to three positron lifetimes are possible to resolve from each measured spectrum. Then a more quantitative analysis of the defect properties can be performed.

In conclusion, visible and invisible damaged areas and the resulting defect structure of a GaAs wafer could be identified with lifetime measurements using the scanning positron microscope. The possibilities of the SPM have been demonstrated. However, the potential power of the system will be achieved when the intense reactor based positron source can be used, which will be possible in the very near future [17–19].

The GaAs wafer has been made available to us by K. Maier.

[1] D. Schödlbauer, P. Sperr, G. Kögel, and W. Triftshäuser, Nucl. Instrum. Methods Phys. Res., Sect. B **34**, 258 (1988).
[2] P. Willutzki *et al.,* Meas. Sci. Technol. **5**, 548 (1994).
[3] P. Sperr, G. Kögel, P. Willutzki, and W. Triftshäuser, Appl. Surf. Sci. **116**, 78 (1997).
[4] D. T. Britton *et al.,* Appl. Phys. A **58**, 389 (1994).
[5] P. Willutzki, J. Störmer, D. T. Britton, and W. Triftshäuser, Appl. Phys. A **61**, 321 (1995).
[6] W. Bauer-Kugelmann *et al.,* Appl. Surf. Sci. **116**, 231 (1997).
[7] X. Y. Zhou, W. Bauer-Kugelmann, J. Störmer, G. Kögel, and W. Triftshäuser, Phys. Lett. A **225**, 143 (1997).
[8] W. Bauer-Kugelmann, G. Kögel, P. Sperr, and W. Triftshäuser, Mater. Sci. Forum **225-257**, 662 (1997).
[9] W. Triftshäuser, Vacuum **58**, 33 (2000).
[10] A. Zecca *et al.,* Europhys. Lett. **29**, 617 (1995).
[11] K. Uhlmann *et al.,* Fresenius' J. Anal. Chem. **353**, 594 (1995).
[12] W. Triftshäuser *et al.,* Nucl. Instrum. Methods Phys. Res., Sect. B **130**, 264 (1997).
[13] D. T. Britton, K. Uhlmann, and G. Kögel, Appl. Surf. Sci. **85**, 158 (1995).
[14] K. F. Canter *et al.,* in *Atomic Physics with Positrons,* edited by J. W. Humberton and E. A. G. Armour (Plenum Press, New York, 1987), p. 153.
[15] R. Krause-Rehberg and H. S. Leipner, *Positron Annihilation in Semiconductors* (Springer, Berlin, Heidelberg, New York, 1998), p. 279.
[16] J. Gebauer *et al.,* Mater. Sci. Forum **255-257**, 204 (1997).
[17] W. Triftshäuser, Acta Phys. Hung. **75**, 61 (1994).
[18] G. Triftshäuser *et al.,* Mater. Sci. Forum **175-178**, 221 (1995).
[19] C. Hugenschmidt *et al.,* Appl. Surf. Sci. **149**, 7 (1999).